An algorithmic method for functionally defining regions of interest in the ventral visual pathway

Citation: Julian, J.B., Evelina Fedorenko, Jason Webster, and Nancy Kanwisher. "An Algorithmic Method for Functionally Defining Regions of Interest in the Ventral Visual Pathway." NeuroImage 60, no. 4 (May 2012): 2357–2364.

As Published: http://dx.doi.org/10.1016/j.neuroimage.2012.02.055

Publisher: Elsevier

Persistent URL: http://hdl.handle.net/1721.1/102470

Version: Author's final manuscript: final author's manuscript post peer review, without publisher's formatting or copy editing

An algorithmic method for functionally defining regions of interest in the ventral visual pathway

J. B. Julian[1], Evelina Fedorenko[1], Jason Webster[2] & Nancy Kanwisher[1]

1. McGovern Institute for Brain Research, Massachusetts Institute of Technology, Cambridge, Massachusetts, 02139, United States of America

2. Department of Psychology, The University of Washington, Seattle, Washington, 98195, United States of America

Corresponding author and address (including email and phone number):
Joshua B. Julian
McGovern Institute for Brain Research
MIT
43 Vassar Street, 46-4141
Cambridge, MA 02139
jjulian@mit.edu
(617) 258-0670

Number of figures and tables: 5 figures; 2 tables

Contents of supplemental material: 2 supplemental figures, 1 supplemental table

Number of pages: 9

Number of words: Abstract = 143; Main Text = 4,364

Six keywords:
fMRI, Group-Constrained Subject-Specific (GSS), high-level vision, ROI, subjectivity, category-selectivity

Acknowledgments:
We would like to thank the Athinoula A. Martinos Imaging Center at the McGovern Institute for Brain Research, MIT, Cambridge, MA. We would also like to thank David Pitcher and Daniel Dilks for data collection and defining fROIs, and Jia Liu, Chris Baker, and Russell Epstein for defining fROIs. This work was supported by a grant from the Ellison medical Foundation to NK.

Abstract
In a widely used functional magnetic resonance imaging (fMRI) data analysis method, functional regions of interest (fROIs) are handpicked in each participant using macroanatomic landmarks as guides, and the response of these regions to new conditions is then measured. A key limitation of this standard handpicked fROI method is the subjectivity of decisions about which clusters of activated voxels should be treated as the particular fROI in question in each subject. Here we apply the Group-Constrained Subject-Specific (GSS) method for defining fROIs, recently developed for identifying language fROIs (Fedorenko et al., 2010), to algorithmically identify fourteen well-studied category-selective regions of the ventral visual pathway (Kanwisher, 2010). We show that this method retains the benefit of defining fROIs in

individual subjects without the subjectivity inherent in the traditional handpicked fROI approach. The tools necessary for using this method are available on our website (http://web.mit.edu/nklab/GSS).

Introduction

In a common approach to analyzing functional magnetic resonance imaging (fMRI) data, functional regions of interest (fROIs) are defined independently in each participant, and those regions are then probed further to determine their precise function. Despite the many advantages of this approach (Nieto-Castañon et al., submitted; Saxe et al., 2006a), a key limitation is the subjective nature of the choice of which activation cluster should count as the fROI in question in each subject. Such decisions are often made by human data coders guided by macroanatomical landmarks (e.g., gyri and sulci) and stereotaxic coordinates from published studies. However, because of variability across individuals in fROI locations and the lack of a clear mapping between function and cortical structure, these constraints do not always provide clear and unique solutions (Nieto-Castañon et al., 2003). For example, even for well-characterized functional regions like the fusiform face area (FFA), expert data coders may sometimes disagree about whether a given cluster of face-selective voxels constitutes the FFA or the more posterior occipital face area (OFA), or whether the FFA should include two nearby but not contiguous clusters in a given individual (Weiner & Grill-Spector, 2010) or just one of these (and if the former, which one?). Of course, procedures are sometimes put in place to eliminate these judgment calls, such as choosing only activated voxels that land within a sphere of a given radius around a published activation peak. Any such algorithmic procedure will eliminate experimenter biases in fROI selection, and adoption of a common method across labs will enable replication and direct comparison of results from different labs. But ideally the convention so adopted would be a principled one. Here we propose a particular algorithmic solution for defining fROIs in the ventral pathway that is based on not only the peaks or centroids of activation across subjects for each fROI, but their shape, spatial extent, and anatomical variability across subjects. Importantly, this method does not require strict voxelwise anatomical overlap of fROIs across subjects.

The Group-Constrained Subject-Specific (GSS) method was originally developed for identifying functional regions of interest engaged in high-level language processing (Fedorenko, et al., 2010). This method was designed to discover regions that are activated most systematically across subjects and– crucially– to define the borders around and between each of these regions. Guided by the spatial distribution of individual activations in a set of subjects, this method identifies key "parcels" within which most subjects show activation for the contrast of interest. The selection of individual subject fROIs is then accomplished by intersecting each individual subject's localizer activation map with each of the parcels, thus defining fROIs in each individual subject in a fully algorithmic fashion. We test here how well this method identifies well-established fROIs in the ventral visual pathway. Specifically, we use the GSS method to define face, scene, body, and object selective fROIs in visual cortex, and we compare these fROIs to handpicked regions of interest defined by expert human data coders on the same data. We show that the GSS method is able to identify known category-selective fROIs in visual cortex, and that such fROIs are spatially and functionally similar to those defined using the traditional handpicked approach. Thus, the GSS method retains the benefit of defining fROIs within

individual subjects while avoiding the subjectivity common in the traditional individual-subjects fROI methodology. The major category-selective group-level parcels resulting from the GSS analyses on a set of 30 subjects are available online (http://web.mit.edu/bcs/nklab/GSS) along with instructions and software, so that other labs can easily use these parcels to define individual-subject fROIs in the same fashion.

Methods

Participants. Thirty-five participants (15 males, mean age 23, range 18-36) were recruited from the Boston area for this experiment. All participants had good visual acuity, and were free of ophthalmic, neurologic, and general health problems. Participants provided informed consent in accordance with the Internal Review Board at the Massachusetts Institute of Technology.

Design. A blocked fMRI design was used in which participants viewed three-second movie clips of faces, bodies, scenes, objects and scrambled objects (Pitcher et al., 2011). The face and body movies were filmed on a black background, and consisted of children dancing and playing. Each body movie showed a portion of the body other than the face (e.g. feet and legs, hands). Scene stimuli consisted mostly of pastoral scenes, although other types of scene movies (e.g., walking in a cave) were included for variety. For the object movies, different moving objects were filmed against a black background (e.g., a ball rolling down an inclined plane). Scrambled objects were constructed by dividing each object movie clip into a 15 by 15 box grid and spatially rearranging the location of each of the resulting movie frames. Each subject completed four runs. Each run was 234 seconds long and consisted of two blocks per stimulus category. The order of the stimulus category blocks in each run was palindromic (e.g., fixation, faces, objects, scenes, bodies, scrambled objects, fixation, scrambled objects, bodies, scenes, objects, faces, fixation) and was randomized across runs. Each block contained six movie clips from the same category for a total of 18 seconds per block. We also included 18-second rest blocks at the beginning, middle, and end of each run, during which time the screen alternated between different full-screen colors once every three seconds (0.3 Hz).

Data Acquisition. Scanning was performed using a 3T Siemens Trio scanner with a 32-channel head coil at the Athinoula A. Martinos Imaging Center at the McGovern Institute for Brain Research at MIT. Functional blood oxygen-level dependent (BOLD) images were acquired with a gradient-echo EPI sequence (TR = 2,000 ms; TE = 30 ms, FOV = 192 x 192, matrix = 64 x 64, slices = 32) with a 3 x 3 x 3.6 mm voxel resolution. Slices were oriented approximately parallel to the calcarine sulcus and provided whole-brain coverage. High-resolution T1-weighted structural images were collected in 128 axial slices with 1.33 mm isotropic voxels (TR = 2,000 ms, TE = 3.39 ms).

Initial fMRI Data Analyses. MRI data were analyzed using SPM5 (www.fil.ion.ucl.ac.uk/spm/software/spm5) and custom software for MATLAB (http://www.mathworks.com/products/matlab/). Each subject's data were motion corrected, normalized to a common brain template (the MNI EPI template), spatially smoothed using a Gaussian filter (FWHM = 6 mm), and then modeled using a box-car regressor. Next, four contrasts were computed for each participant: faces > objects, scenes > objects, bodies > objects, and objects > scrambled. Because we wanted to

later examine the response profiles of the resulting fROIs in an independent subset of the data (see Kriegeskorte et al., 2009; Vul & Kanwisher, 2010)), we excluded the first functional run from these contrasts, and defined fROIs using the remaining three runs. All activation maps were thresholded at $p < 0.0001$, uncorrected, prior to further analyses. A threshold of $p < 0.0001$ was chosen because it has been used in numerous previous reports on ventral visual stream fROIs (e.g., Downing et al., 2001; Epstein & Kanwisher, 1998; Grill-Spector et al., 2004; Kanwisher et al., 1997; Spiridon et al., 2006; Yovel & Kanwisher, 2005).

Group-Constrained Subject-Specific Method. The data from 30 of the 35 subjects were used for the main GSS analysis. The GSS method starts after the initial analyses described above and consists of four steps. First, for each contrast of interest, individual subjects' binary activation maps (thresholded $p < 0.0001$, uncorrected) were overlaid on top of one another in common stereotaxic (MNI) space. The result of this step was a probabilistic overlap map for each contrast of interest (i.e., faces > objects, scenes > objects, bodies > objects, and objects > scrambled) (Figure 1.1, Supplemental Figure 1 A1-C1). Each voxel in these overlap maps contains information about the number of subjects that have activation in that voxel for a given contrast. Thus, the overlap maps contain information about points of high inter-subject overlap, and also information about the distribution of individual activations around these high overlap points. The overlap maps were spatially smoothed with a Gaussian filter (FWHM = 6mm), and thresholded such that they contained only those voxels that had at least 10% overlap across subjects (i.e., at least 3 subjects had to have activation at a voxel for that voxel to be included in the overlap map).

Second, the overlap maps were divided into group-level "parcels" following the topographical information in the maps, using a watershed image segmentation algorithm (Meyer, 1991), as in Fedorenko et al. (2010). This algorithm finds local maxima and "grows" regions around these maxima by incorporating neighboring voxels in decreasing order of voxel intensity (i.e., the number of subjects showing activation at that voxel). The result of this step was a set of group-level parcels for each contrast of interest (Figure 1.2, Supplemental Figure 1 A2-C2). The faces > objects, scenes > objects, bodies > objects, and objects > scrambled probabilistic overlap maps resulted in 21, 16, 19, and 13 group-level parcels, respectively.

Third, because the overlap map includes voxels that are present in as few as three participants, a number of the parcels identified are small regions specific to only a few subjects. Figure 2 illustrates the relationship between the size of the parcels and the number of subjects that have significantly activated voxels within those parcels. Because we wanted to focus on functional regions present in the majority of subjects, we selected the subset of group-level parcels for which at least 18 out of 30 (i.e., $\geq$ 60%) subjects show some activated voxels within that parcel. See Table 1 for a list of the anatomical locations of all the parcels resulting from this step for each contrast. Because we were primarily interested in determining if the GSS method replicates previous individual fROI studies, of those group-level parcels listed in Table 1, only those parcels that correspond to well-known category-selective fROIs in visual cortex (marked in italics in Table 1) were investigated further. A parcel was considered to correspond to a well-known category-selective fROI if that parcel overlapped with coordinates reported in previous studies on ventral visual stream fROIs.

Fourth, we defined each fROI in each individual subject by intersecting the chosen group-level parcel with that subject's activation map for the relevant contrast (e.g., the parcel corresponding to the FFA was intersected with that subject's faces >

objects map, thresholded at p's < 0.0001) (Figure 1.3, Supplemental Figure 1 A3-C3). In contrast to some standard individual-subject fROI analyses, no constraint of contiguity was placed on the topography of individual subject voxels within the boundaries of the parcels.

In order to i) test how well our group-level parcels pick out relevant functional clusters in new subjects (i.e., subjects who were not used in deriving these parcels), and ii) directly compare the GSS fROIs with the standard handpicked fROIs, we used the parcels discovered from the set of 30 subjects to define GSS fROIs in the remaining 5 subjects. In particular, we intersected the group-level parcels derived from the functional data of 30 participants with the five independent participants' corresponding activation maps. For this analysis, we focused on the four major category-selective fROIs (FFA, PPA, EBA, and LOC) in the right hemisphere, and compared the size and location of these GSS defined fROIs with those defined using the handpicked method. Since these GSS fROIs were defined using all but the first functional run, we extracted response profiles from these regions using independent data, and compared these profiles with those of the standard handpicked analysis.

Traditional Handpicked fROI Method. Following the initial analyses described above, the five subjects not included in the GSS analysis were analyzed using the traditional individual-subjects fROI approach. For these five participants, expert human data coders from three different labs specializing in the ventral visual pathway were asked to define the best-established face, scene, body, and object-selective fROIs (one such fROI per contrast) in ventral visual cortex. Each fROI was defined by three unique human data coders. The main face-selective region, the Fusiform Face Area (FFA), was defined from the faces > objects contrast. The scene-selective region, the Parahippocampal Place Area (PPA), was defined based on the scenes > objects contrast. The body-selective region, the Extrastriate Body Area (EBA), was defined from the bodies > objects contrast. Finally, the object-selective region, the Lateral Occipital Complex (LOC), was defined from the objects > scrambled contrast. Each fROI was defined in the right hemisphere. To define these regions, data coders were shown contrast maps overlaid on 48 horizontal slices of a standard MNI template and were asked to indicate slice-by-slice which activation cluster corresponded to each of the key fROIs for that contrast. The data coders' fROI selections were then converted to binary masks using custom scripts for MATLAB. Because we defined fROIs using activation maps for all but the first functional run, we were able to later examine response profiles of these regions using independent data.

Results

Using the GSS method to identify known category-selective fROIs.
Table 1 shows the percent of subjects used to define the parcels in whom each of the best-established ventral pathway fROIs was identified in each hemisphere. First, from the faces > objects contrast, the GSS method successfully identified the main face-selective regions in the right hemisphere: the Fusiform Face Area (FFA) in 93% of subjects, Occipital Face Area (OFA) in 75% of subjects, and posterior Superior Temporal Sulcus (pSTS) in 93% of subjects. The GSS method also identified other fROIs from the faces > objects contrast present in a smaller percentage of subjects that are known to exhibit face selectivity, including left hemisphere homologues of the FFA, OFA, and pSTS, the right inferior frontal gyrus (rIFG) (e.g., Chan et al.,

2006), orbitofrontal cortex (e.g., Rolls, 1999), and the right middle Superior Temporal Sulcus (rmSTS) (Pitcher et al., 2011). Second, from the scenes > objects contrast the GSS method successfully identified the best known scene-selective regions: the Parahippocampal Place Area (PPA) and Retrosplenial Cortex (RSC), each in 90% of subjects in the right hemisphere, and the right Transverse Occipital Sulcus (TOS) in 74% of subjects. Third, from the bodies > objects contrast the GSS method identified the bilateral body-selective Extrastriate Body Area (EBA) in 93% of subjects in each hemisphere. Finally, from the objects > scrambled contrast the GSS method identified the object-selective region, Lateral Occipital Complex (LOC), in 97% of right hemispheres and 93% of left. These findings indicate that the GSS method can successfully identify the major category selective regions in ventral visual cortex in a totally data-driven fashion.

All major category-selective fROIs identified by the GSS method were located in typically reported stereotaxic locations and were of standard size (Table 1). Moreover, when the key GSS-defined individual subject fROIs were used to extract response profiles from an independent set of data (i.e., the first run), we found that these regions exhibited the expected response profiles (Figure 3, Supplemental Figure 2). In particular, for each fROI, a 5-level (stimulus category: faces, bodies, scenes, objects, scrambled objects) repeated-measures ANOVA revealed a main effect of category (all F's > 40, all p's < 0.001), with every fROI except LOC responding significantly more to its preferred stimulus category than any other category (Main Effect contrasts, all p's < 0.001). The LOC responded significantly more strongly to both objects and bodies than any other category (Main Effect contrasts, all p's<0.001), consistent with previous reports (Saxe et al., 2006b). Lastly, unlike in the handpicked method in which a fROI is typically defined as a contiguous cluster of activation, the GSS method did not impose any contiguity constraints, making it possible for the GSS-defined fROIs to consist of multiple distinct clusters of activation. However, even though no explicit contiguity constraint was imposed on the fROIs, a detailed examination of the fROIs revealed that most individual fROIs consisted of a single large cluster of activated voxels. In particular, on average, at least 89% of voxels in each of the major category-selective fROIs was captured by the largest contiguous cluster within a given parcel (Table 1). To summarize, because the GSS method identified fROIs in the standard locations, of the standard sizes, location, and form, and that exhibit the typical response profiles, we conclude that the GSS method identified known category-selective fROIs.

Note that the above analyses were performed on spatially smoothed (FWHM = 6 mm) individual subject data. Is this spatial smoothing necessary to identify the major category selective fROIs? To investigate this question, we reran the above analyses on unsmoothed data. Using unsmoothed data, the faces > objects, scenes > objects, bodies > objects, and objects > scrambled probabilistic overlap maps resulted in 12, 15, 5, and 19 group-level parcels, respectively. Supplemental Table 1 shows the percent of subjects used to define the parcels in whom each of the ventral pathway fROIs were identified based on unsmoothed data. The results were similar to those resulting from the smoothed analysis. In particular, the GSS method identified the major category selective fROIs in the ventral visual stream in the majority of subjects: FFA, OFA, pSTS from the faces > objects contrast, PPA, RSC, TOS from the scenes > objects contrast, EBA from the bodies > objects contrast, and LOC from the objects > scrambled contrast bilaterally. These fROIs were located in typically reported stereotaxic locations and were of standard size for unsmoothed analyses (Supplemental Table 1). Thus, spatial smoothing of the individual subject data is not

necessary to identify the major category-selective fROIs in the ventral visual stream using the GSS method.

Comparison Between the Traditional Handpicked and GSS Methods
Will the parcels derived here generalize to a new set of subjects who were not included in the set used to derive the parcels? Further, how well do the parcels derived with this method match those derived from individual handpicked methods? To answer this question, the fROIs defined in an independent set of participants (i.e., in the five participants that were not included in the set of subjects who were used to make the group-level parcels) by three expert human data coders were similar to those defined by the GSS method in terms of volume and location (Table 2). Both the GSS and three human data coders agreed that one independent subject had non-significant localizer results for the PPA. Finally, response profiles extracted from an independent subset of the data for the GSS-defined independent participants were similar to those of the correspondingly handpicked fROIs (Figure 4), as expected given the high degree of overlap across the fROIs. Thus, the GSS method identified known category-selective fROIs in ventral visual cortex, and the voxels so chosen are highly overlapping with those identified by the traditional handpicked individual subjects fROI method.

Further refinements
Although the GSS method identified the major category selective regions for each contrast of interest, it has been argued in the literature that some of these regions are composed of spatially segmented subregions. For example, the LOC has been argued to consist of LO, a dorsal-caudal subdivision, and the posterior Fusiform sulcus (pFs; Grill-Spector et al., 2001), a ventral-anterior subdivision located in the fusiform gyrus. Similarly, some have suggested that the FFA consists of two spatially distinct clusters (e.g., FFA-1/2; Pinsk et al., 2009; Weiner & Grill-Spector, 2010). To see if the GSS method could be used to identify these fROI subregions, we spatially smoothed the overlap map using a smaller Gaussian smoothing kernel (FWHM = 3mm, instead of 6mm) to reduce the extent of voxelwise overlap in the overlap map, and reran the above analyses. By decreasing the amount of smoothing of the overlap map, the LOC was successfully divided into LO and pFs (Figure 5). Both the LO and pFs fROIs resulting from this new division were identified in most subjects (96% and 85% of subjects in the right hemisphere, and 92% and 85% in the left hemisphere, for LO and pFs, respectively). Moreover, by decreasing the amount of smoothing of the overlap map the GSS method also successfully identified two distinct right FFA parcels, one more anterior than the other, as in Weiner et al. (2010) (Figure 5). Half of subjects (47%) had activation in both FFA parcels, 29% had activation in the anterior parcel only, and 17% had activation only in the more posterior parcel. Note that some of the participants that had activation in both FFA parcels exhibited only a single activation cluster that was subsequently bisected by the boundary between the two FFA parcels. These findings demonstrate that by adjusting the size of the overlap smoothing kernel, the GSS method can be used to identify subdivisions within larger regions as long as the spatial locations of these subregions are relatively consistent across subjects. Of course, for any contrast of interest, the extent to which such subregions are functionally distinct remains an open question. However, given that the GSS method can be used successfully for defining fROI subregions, future experiments can determine whether or not such regions should be treated as distinct functional units.

Discussion

The data presented show that the algorithmic GSS method described here is highly effective in quickly and reliably identifying in individual subjects each of the main face, scene, body, and object perception fROIs in the ventral visual pathway. This method avoids the subjectivity inherent in choosing fROIs by hand, yet identifies regions that closely match the intuitions of human data coders. The major category-selective group-level parcels resulting from the GSS analyses discussed here are available online (http://web.mit.edu/bcs/nklab/GSS); researchers can use these parcels and their own localizer data to identify fROIs using the methods described here.

While other procedures exist to similarly reduce the subjectivity of the handpicked fROI method, the GSS method has some advantages over these procedures. First, in contrast to the use of spheres defined around published group fROI centroids to constrain the fROI choice in each subject, the GSS method exploits the fact that actual fROIs are not spheres but have characteristic irregular shapes. Second, rather than having to choose an arbitrary radius for the sphere, the GSS method follows the data to define fROI borders where they most often fall across a group of subjects. Third, in contrast to the use of a group fROI from a prior published study (or from an analysis of an independent set of data from the same subjects), the GSS method allows identification of fROIs in some subjects that may be adjacent to but not overlapping with fROIs in other subjects.

Further, because parcels contain information about what proportion of individuals show a particular functional characteristic within the parcel boundaries, another advantage of the GSS method is that the resulting parcels can be used in a similar way to probabilistic cytoarchitecture maps (e.g., Amunts et al., 1999). Specifically, for any activation cluster identified in a functional imaging study, or for a lesion in a patient, we can determine the likelihood that each voxel within the activation cluster / lesion would have a particular functional characteristic (e.g., a greater response to faces than objects) based on whether or not it falls within certain parcel boundaries. Thus, rather than correlating an activation cluster or a lesion with structural (e.g., cytoarchitectonic) information, as in Amunts et al. (1999), activation clusters / lesions could be correlated with functional information derived from the GSS method to provide insights into the function of that cortical region.

Other research groups have recently begun developing probabilistic functional atlases. For example, Frost & Goebel (2011) provide probabilistic functional maps for several key functional regions. These maps can be used in analogous ways to our parcels. In particular, the boundaries of these functional regions can serve to algorithmically constrain the selection of relevant functional voxels for each individual subject in defining subject-specific fROIs. Note, however, that Frost & Goebel's (2011) functional maps are group-based, and these researchers have not discussed the crucial method proposed here of determining each individual subject's fROI based on the group maps. One benefit of Frost & Goebel's maps is that they can be used for surface-based analyses, which generally achieve better inter-subject alignment of activations (e.g., Fischl et al., 2008; Frost & Goebel, 2011). All of the current GSS-style analyses are conducted in the volume, although we plan to extend this work to surface-based analyses in the future.

Finally, note that in principle the GSS method can help answer a broader question than the specific methodological goal discussed so far in this paper. Specifically, beyond simply determining how to best identify fROIs that are already well established in the literature, the GSS method can be used to ask the more fundamental question of which of those fROIs should be considered distinct from each other in the first place. For example, should the FFA be considered two distinct regions (Weiner et al., 2010), and should the OFA be considered as distinct from the FFA? To the extent that the GSS method identifies subdivisions, in which each of these candidate clusters is assigned a distinct parcel, it is essentially answering this question by telling us that these divisions arise from the pattern of activation across subjects. However, the solutions delivered by the GSS method are at least partly dependent on various analysis parameters including i) the statistical threshold for individual activation maps (Duncan & Devlin, 2011), ii) the threshold for the probabilistic overlap map, iii) the size of the spatial smoothing kernel for the overlap map, and iv) the selection criterion for what counts as a 'meaningful' parcel (e.g., the percentage of subjects that must show activation within a parcel boundary for the parcel to be considered in subsequent analyses). The strongest solutions will be those that are most robust to changes in these parameters. Finally, the GSS method can only discover parcels where activations across subjects overlap at least somewhat. Thus, systematic patterns that do not produce any consistent overlap across subjects will not be reliably identified by this method. For example, imagine a functional localizer that identifies two clearly distinct clusters in each subject individually, but the location of those two clusters varies so much across subjects that the GSS method can find only one big low-overlap cluster. Ongoing work is attempting to develop a more powerful language for describing activations and their relative locations in the brain that can reveal even this more abstract (but still functionally consistent) spatial structure.

Amunts, K., Schleicher, A., B¸rgel, U., Mohlberg, H., Uylings, H., & Zilles, K. (1999). Broca's region revisited: cytoarchitecture and intersubject variability. *The Journal of comparative neurology, 412*(2), 319-341.

Chan, A.W.Y., Peelen, M.V., & Downing, P.E. (2006). An exploration of face selectivity in human inferior frontal cortex. *Journal of Vision, 6*(6), 663.

Downing, P.E., Jiang, Y., Shuman, M., & Kanwisher, N. (2001). A cortical area selective for visual processing of the human body. *Science, 293*(5539), 2470.

Duncan, K.J.K., & Devlin, J.T. (2011). Improving the reliability of functional localizers. *Neuroimage*.

Epstein, R., & Kanwisher, N. (1998). A cortical representation of the local visual environment. *Nature, 392*(6676), 598-601.

Fedorenko, E., Hsieh, P.J., Nieto-Castañon, A., Whitfield-Gabrieli, S., & Kanwisher, N. (2010). New method for fMRI investigations of language: Defining ROIs functionally in individual subjects. *Journal of neurophysiology, 104*(2), 1177.

Fischl, B., Rajendran, N., Busa, E., Augustinack, J., Hinds, O., Yeo, BT, . . . Zilles, K. (2008). Cortical folding patterns and predicting cytoarchitecture. *Cerebral Cortex, 18*(8), 1973.

Frost, M.A., & Goebel, R. (2011). Measuring Structural-Functional Correspondence: Spatial variability of specialised brain regions after macro-anatomical alignment. *Neuroimage*.

Grill-Spector, K., Knouf, N., & Kanwisher, N. (2004). The fusiform face area subserves face perception, not generic within-category identification. *nature neuroscience, 7*(5), 555-562.

Grill-Spector, K., Kourtzi, Z., & Kanwisher, N. (2001). The lateral occipital complex and its role in object recognition. *Vision research, 41*(10-11), 1409-1422.

Kanwisher, N. (2010). Functional specificity in the human brain: a window into the functional architecture of the mind. *Proceedings of the National Academy of Sciences, 107*(25), 11163.

Kanwisher, N., McDermott, J., & Chun, M.M. (1997). The fusiform face area: a module in human extrastriate cortex specialized for face perception. *The Journal of Neuroscience, 17*(11), 4302.

Kriegeskorte, N., Simmons, W.K., Bellgowan, P.S.F., & Baker, C.I. (2009). Circular analysis in systems neuroscience: the dangers of double dipping. *nature neuroscience, 12*(5), 535.

Meyer, Fernand. (1991). *Un algorithme optimal pour la ligne de partage des eaux.* Paper presented at the Dans 8me congrès de reconnaissance des formes et intelligence artificielle, Lyon, France.

Nieto-Castañon, Ghosh, S.S., Tourville, J.A., & Guenther, F.H. (2003). Region of interest based analysis of functional imaging data. *Neuroimage, 19*(4), 1303-1316.

Nieto-Castañon, Kanwisher, N. , & Fedorenko, E. . (submitted). Subject-specific functional localizers increase sensitivity and functional resolution of multi-subject analyses.

Pinsk, M.A., Arcaro, M., Weiner, K.S., Kalkus, J.F., Inati, S.J., Gross, C.G., & Kastner, S. (2009). Neural representations of faces and body parts in macaque and human cortex: a comparative FMRI study. *Journal of neurophysiology, 101*(5), 2581.

Pitcher, D., Dilks, D.D., Saxe, R.R., Triantafyllou, C., & Kanwisher, N. (2011). Differential selectivity for dynamic versus static information in face-selective cortical regions. *Neuroimage*.

Rolls, E.T. (1999). The functions of the orbitofrontal cortex. *Neurocase, 5*(4), 301-312.

Saxe, R., Brett, M., & Kanwisher, N. (2006a). Divide and conquer: a defense of functional localizers. *Neuroimage, 30*(4), 1088-1096.

Saxe, R., Jamal, N., & Powell, L. (2006b). My body or yours? The effect of visual perspective on cortical body representations. *Cerebral Cortex, 16*(2), 178.

Spiridon, M., Fischl, B., & Kanwisher, N. (2006). Location and spatial profile of category specific regions in human extrastriate cortex. *Human Brain Mapping, 27*(1), 77-89.

Vul, E., & Kanwisher, N. (2010). *Begging the question: The non-independence error in fMRI data analysis*: MIT Press: Cambridge, MA.

Weiner, K.S., & Grill-Spector, K. (2010). Sparsely-distributed organization of face and limb activations in human ventral temporal cortex. *Neuroimage, 52*(4), 1559-1573.

Yovel, G., & Kanwisher, N. (2005). The neural basis of the behavioral face-inversion effect. *Current Biology, 15*(24), 2256-2262.

Table 1

Table 1. Results from the main GSS method analysis. Regions in italics were considered in further analyses. If the GSS method did not identify a particular fROI for a given participant, the volume of that participant's fROI was set to 0 for that region. Further, that participant was tallied as lacking that fROI for our calculations of how many subjects showed each fROI; see column 2. Regions are listed from most posterior to anterior. RH = right hemisphere, LH = left hemisphere.

Faces > Objects

Region Name	Percent Subjects	Parcel Size (mm^3)	Average Individual fROI Size (mm^3)	Location of Peak Overlap (MNI)	Average Percent of Activation Captured by Largest Cluster
Early Visual Cortex (incl. Calcarine Sulcus, Lingual Gyrus, Cuneus)	83%	19688	2048	-2 -92 14	88%
Middle Occipital (RH) – rOFA	75%	6320	640	44 -76 -12	92%
Middle Occipital (LH) – lOFA	70%	1688	160	-40 -76 -18	95%
Fusiform Gyrus (LH) – lFFA	63%	4248	416	-40 -52 -18	93%
Fusiform Gyrus (RH) – rFFA	93%	8152	928	38 -42 -22	90%
Posterior Superior Temporal Sulcus (RH) – rpSTS	93%	20040	2400	48 -38 4	88%
Posterior Superior Temporal Sulcus (LH) – lpSTS	70%	6752	648	-54 -38 6	96%
Middle Superior Temporal Sulcus (RH) – rmSTS	60%	1464	144	52 -2 -16	94%
Inferior Frontal Gyrus (RH) – rIFG	67%	1192	104	46 34 2	94%
Orbitofrontal Cortex	63%	10808	968	4 56 24	99%

Scenes > Objects

Region Name	Percent Subjects	Parcel Size (mm^3)	Average Individual fROI Size (mm^3)	Location of Peak Overlap (MNI)	Average Percent of Activation Captured by Largest Cluster
Early Visual Cortex (incl. Calcarine Sulcus, Lingual Gyrus, Cuneus)	100%	90648	22912	-6 -88 -4	87%
Transverse Occipital Sulcus (RH) – rTOS	74%	2008	336	36 -80 20	96%
Transverse Occipital Sulcus (LH) – lTOS	67%	1064	192	-32 -76 24	97%
Retrosplenial Cortex (LH) – lRSC	82%	13298	2776	-10 -54 12	90%
Retrosplenial Cortex (RH) – rRSC	90%	8504	1680	16 -50 6	93%
Parahippocampal Gyrus (RH) – rPPA	90%	4424	864	22 -42 -12	94%

Parahippocampal Gyrus (LH) – lPPA	82%	5856	1200	-20 -42 -12	95%

Bodies > Objects

Region Name	Percent Subjects	Parcel Size (mm^3)	Average Individual fROI Size (mm^3)	Location of Peak Overlap (MNI)	Average Percent of Activation Captured by Largest Cluster
Middle Temporal Gyrus (LH) – lEBA	93%	17204	1992	-48 -74 10	93%
Middle Temporal Gyrus (RH) – rEBA	93%	19304	2536	50 -70 2	89%

Objects > Scrambled

Region Name	Percent Subjects	Parcel Size (mm^3)	Average Individual fROI Size (mm^3)	Location of Peak Overlap (MNI)	Average Percent of Activation Captured by Largest Cluster
Precuneus (LH)	83%	9656	1984	-20 -80 34	86%
Precuneus (RH)	83%	15784	1152	28 -74 38	90%
Lateral Occipital (LH) – lLOC	93%	39768	9864	-46 -72 -4	91%
Lateral Occipital (RH) – rLOC	97%	40680	10296	46 -70 -4	97%
Superior Parietal Lobule (LH)	87%	12720	2680	-24 -56 60	90%
Superior Parietal Lobule (RH)	90%	18912	4584	24 -52 64	90%
Postcentral Gyrus (LH)	83%	9960	2280	-34 -48 58	89%
Postcentral Gyrus (RH)	87%	6280	1312	38 -36 54	87%
Inferior Parietal Lobule & Supramarignal Gyrus (LH)	70%	6544	1160	-56 -32 36	87%
Inferior Parietal Lobule & Supramarignal Gyrus (RH)	67%	6320	1080	58 -24 36	90%

Table 2

Table 2. Comparison between the GSS defined and handpicked fROIs.

	GSS	Data Coder 1	Data Coder 2	Data Coder 3
	Fusiform Face Area (FFA)			
Size (# voxels)	146	149	134	128
Location (MNI)	39 -48 -22	38 -48 -21	38 -47 -21	38 -46 -21
	Parahippocampal Place Area (PPA)			
Size (# voxels)	102	112	82	87
Location (MNI)	22 -44 -14	24 -42 -17	24 -44 -15	24 -46 -14
	Extrastriate Body Area (EBA)			
Size (# voxels)	155	154	122	154
Location (MNI)	48 -70 0	51 -69 -1	50 -69 -1	50 -69 -1
	Lateral Occipital Complex (LOC)			
Size (# voxels)	648	690	680	681
Location (MNI)	48 -67 -14	46 -66 -16	48 -64 -13	48 -66 -15

Figure Legends

Click here to download 9. Figure: figure_legends.doc

Figure 1. The key steps of the group-constrained subject-specific (GSS) method for defining individual subject fROIs illustrated schematically for the faces > objects contrast. The results from each step are shown on 11 horizontal slices of the ventral surface of the brain ranging from z = -24:12. 1) Each individual subject faces > objects activation map is overlaid on top of one another, creating a probabilistic overlap map. Each voxel in the overlap map contains information about the number of subjects that show a significant effect in that voxel (the color of each voxel corresponds to the percentage of subjects that have activation at that voxel). 2) Using a watershed image segmentation algorithm, the overlap map is divided into functional "parcels" following the map's topography. 3) These parcels are then used as spatial constraints to select subject-specific voxels for each region by intersecting each parcel (black outlines) with each individual subjects' thresholded ($p < 0.0001$) faces > objects activation map. The subject-specific fROIs are then defined as the activation that falls within the boundaries of each parcel. Brain images follow the neurological convention (i.e., left is left).

Figure 2. The relationship between the size of the group-level parcels and the number of subjects that have a nonzero intersection in those parcels, collapsed across all contrasts of interest (i.e., for all 77 parcels). The grey bar denotes those parcels considered in further analyses (i.e., those in which greater than or equal to 60% of subjects had significant activation). Note that the x-axis is on a logarithmic scale.

Figure 3. Response profiles for the GSS-defined fROIs (Faces > Objects: FFA, pSTS, OFA; Bodies > Objects: EBA; Scenes > Objects: PPA, RSC, TOS; Objects > Scrambled: LOC) in the right hemisphere. Percent signal change data from the five stimulus categories (faces, bodies, scenes, objects, scrambled objects), compared to fixation baseline, was extracted from an independent set of data. The GSS-defined fROIs exhibit the expected response profiles.

Figure 4. Response profiles for the right hemisphere fROIs (FFA, EBA, PPA, and LOC) defined either by the GSS method or handpicked by expert human data coders for an independent set of subjects (i.e., subjects not included in the original parcels). Percent signal change data from the five stimulus categories (faces, bodies, scenes, objects, scrambled objects), compared to fixation baseline, was extracted from an independent set of data. Note that response profiles for the GSS-defined fROIs were similar to those of the handpicked fROIs.

Figure 5. Further refinements of the GSS defined fROIs in the ventral visual stream. By decreasing the amount of smoothing of the probabilistic overlap map, the GSS method successfully divided the LOC into the oft-used division of LO and pFs (top row), and the right FFA into two discontiguous parcels (FFA-1 and FFA-2) (bottom row). The LO/pFs and FFA-1/2 parcels are shown on three horizontal slices of the ventral surface of the brain ranging from z=-32:-24 and z = -26:-20, for the top and bottom rows respectively. Brain images follow the neurological convention (i.e., left is left).

Figure 1

Click here to download high resolution image

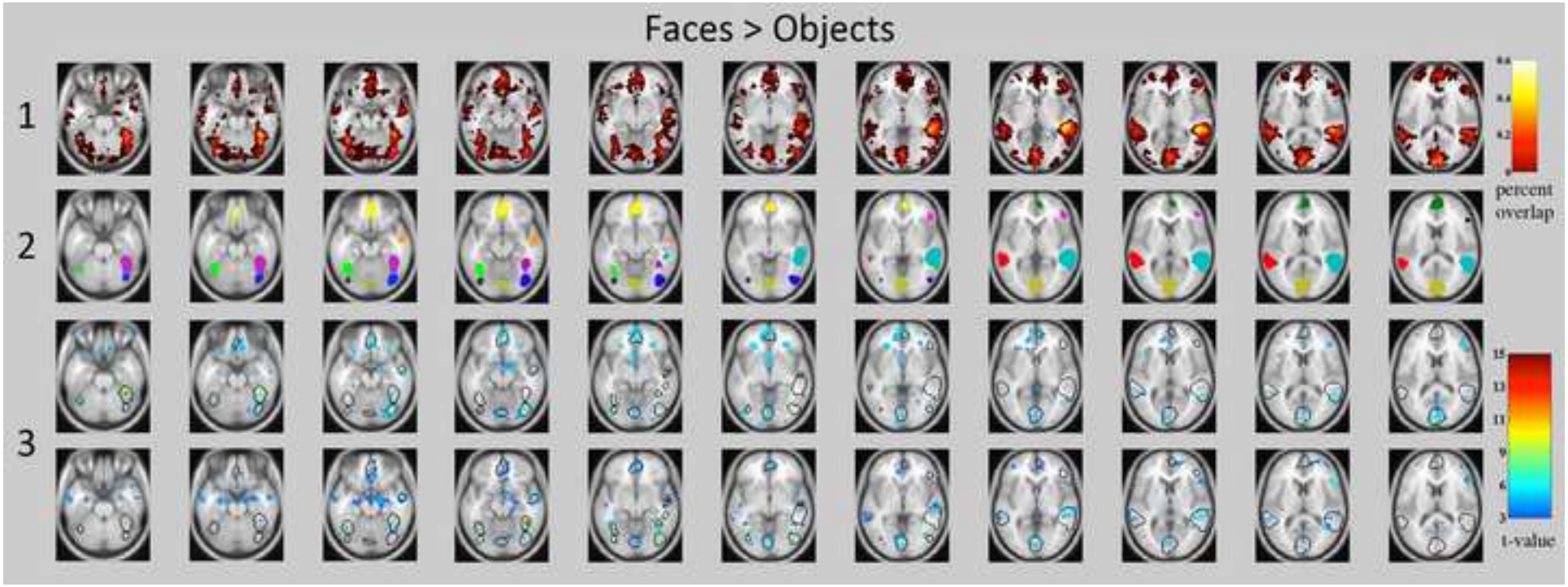

Figure 2

Click here to download high resolution image

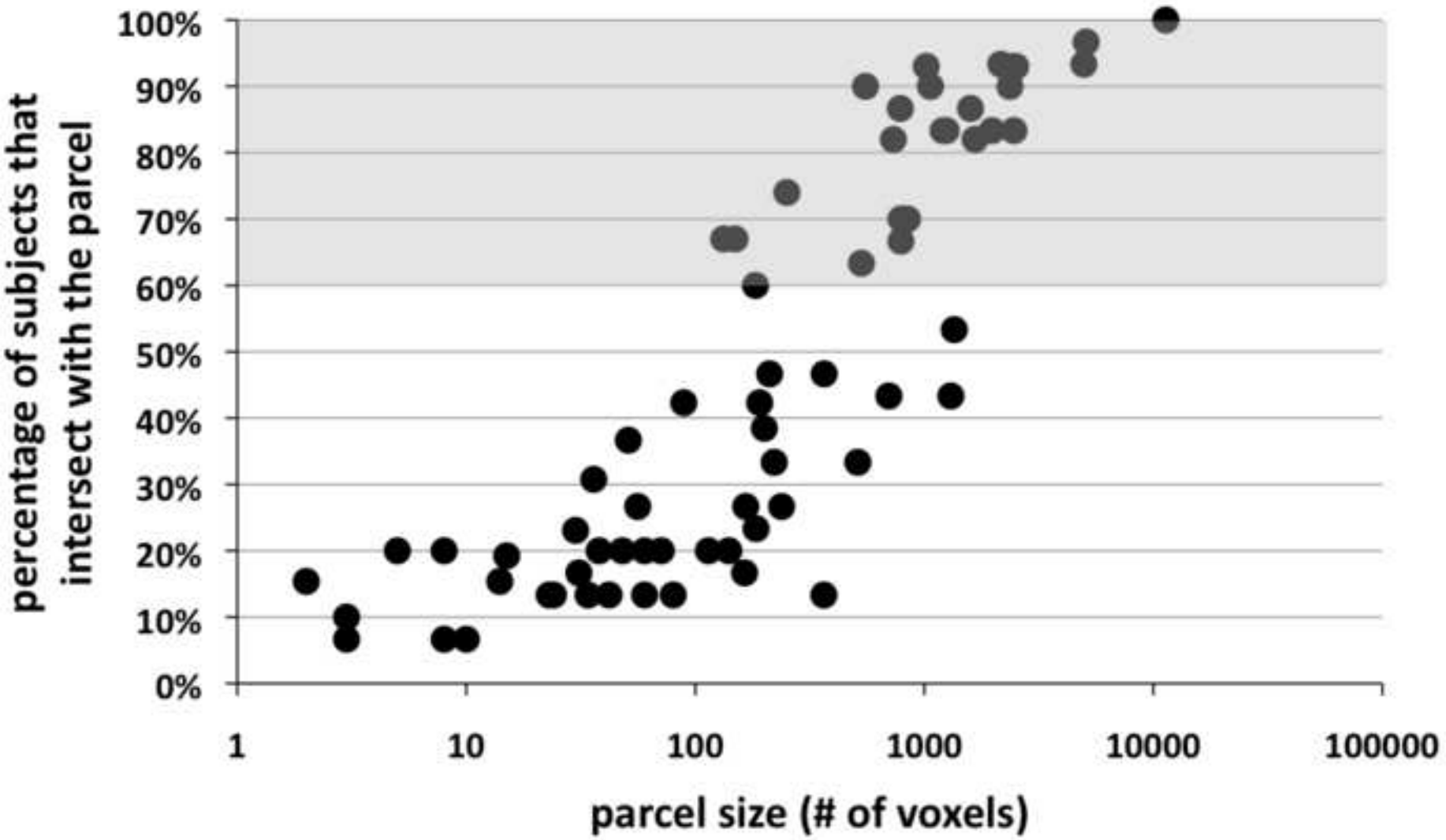

Figure 3
Click here to download high resolution image

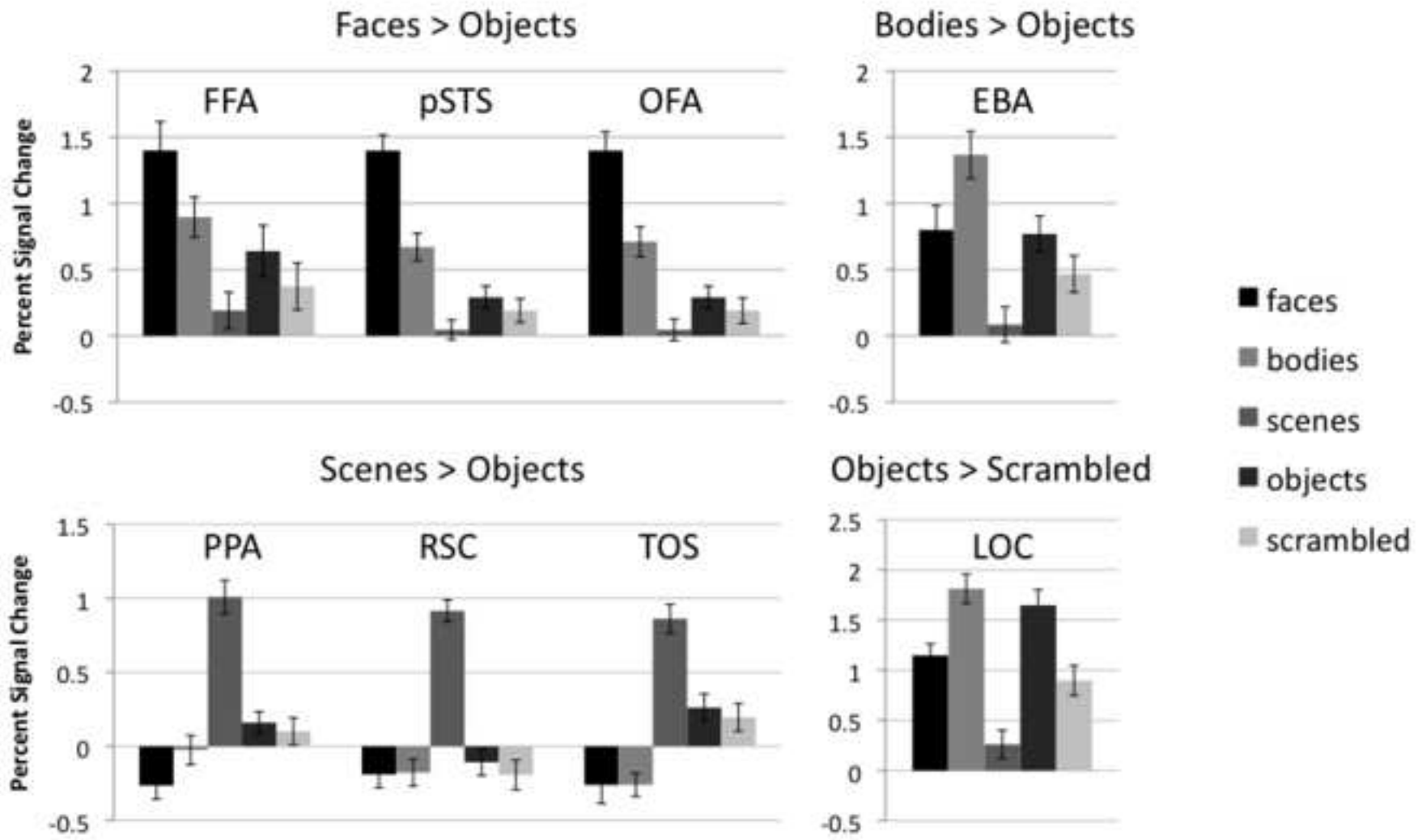

Figure 4

Click here to download high resolution image

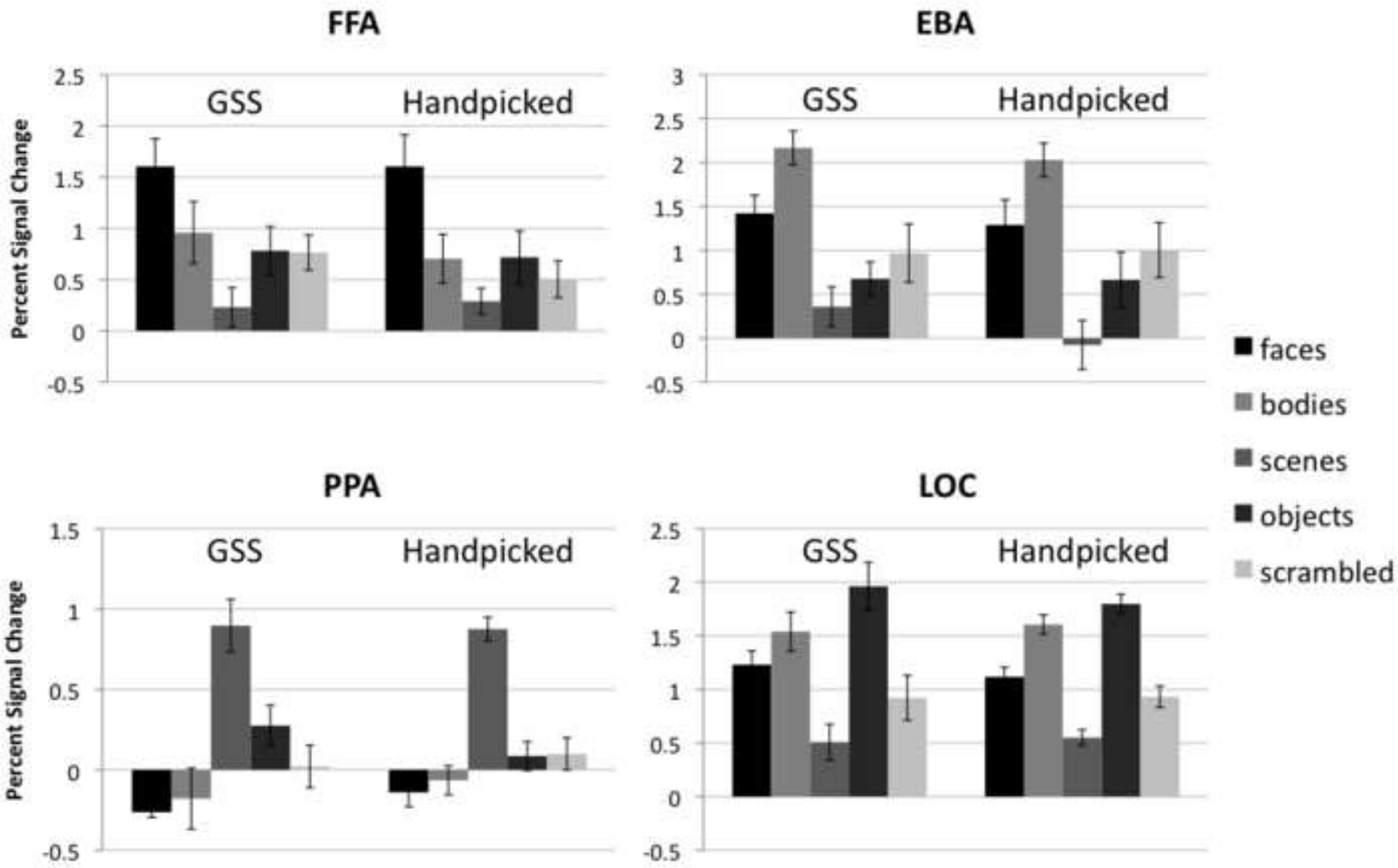

Figure 5

Click here to download high resolution image

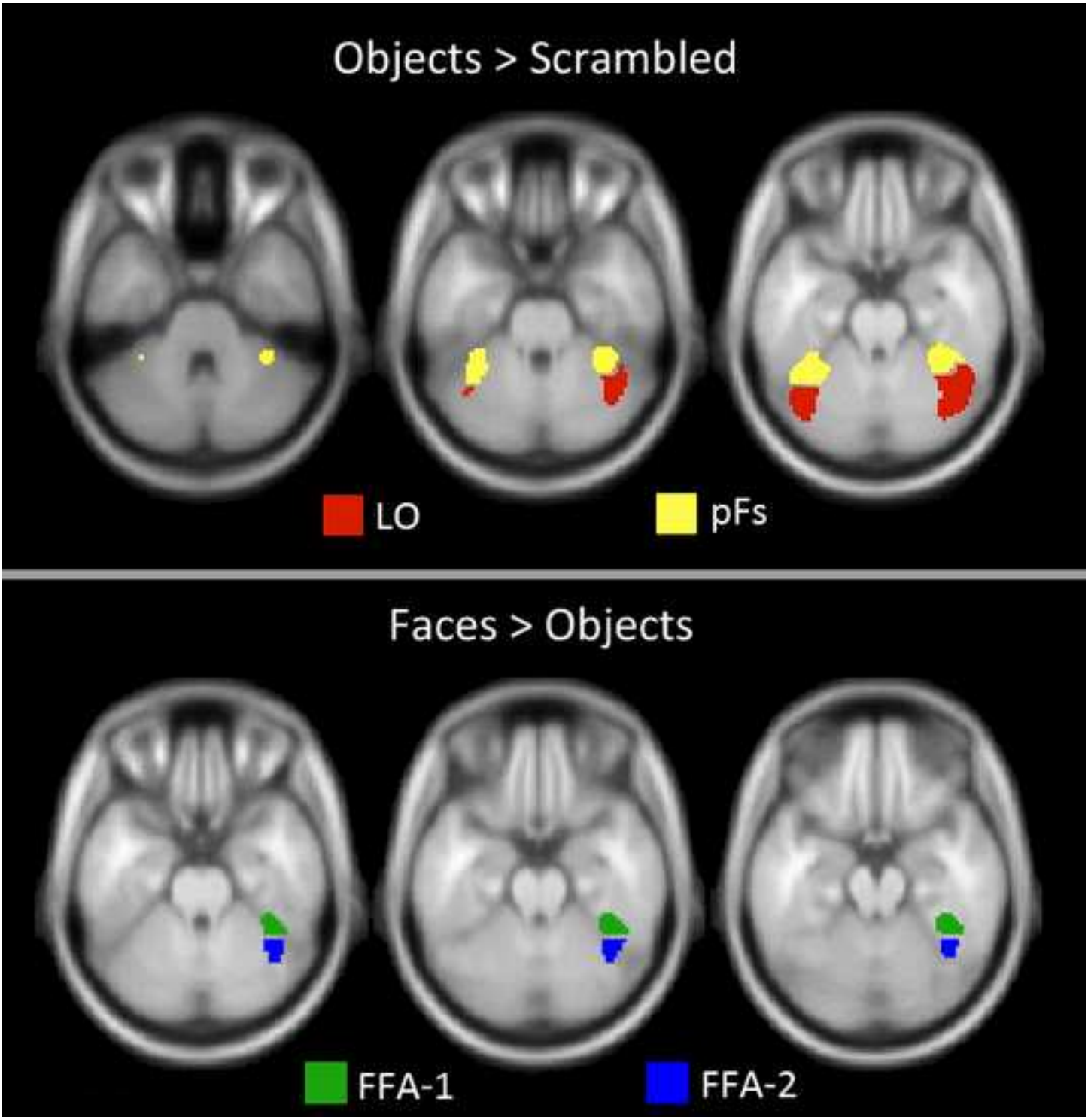

Supplementary Table 1

Click here to download 10. Supplementary Material: Supplemental_Table_1.doc

Supplementary Figure Legend

Click here to download 10. Supplementary Material: supp_figure_legends.doc

Supplementary Figure 1

Click here to download 10. Supplementary Material: Supp_Figure_1.tif

Supplementary Figure 2

Click here to download 10. Supplementary Material: Supp_Figure_2.tif